Research Square

Preprints are preliminary reports that have not undergone peer review.
They should not be considered conclusive, used to inform clinical practice,
or referenced by the media as validated information.

Photoluminescent properties of Eu 3+ , Tb 3+ doped SrWO 4 nanoparticles prepared by ethylene glycol route

Kongbrailatpam Gayatri Sharma

gayatrish83@gmail.com

GP Women's College, Dhanamanjuri University

Research Article

Keywords: Phosphors, Nanoparticles, Photoluminescence, Charge transfer and Rare-earths

Posted Date: April 2nd, 2026

DOI: https://doi.org/10.21203/rs.3.rs-9151142/v1

License: This work is licensed under a Creative Commons Attribution 4.0 International License.
Read Full License

Additional Declarations: No competing interests reported.

Abstract

A series of $SrWO_4$ doped with Eu^{3+} and Tb^{3+} nanoparticles were prepared by co-precipitation method using ethylene glycol as the solvent yielding highly crystalline phosphors.

The phosphors were characterized by the X-ray diffraction (XRD), FT-IR spectroscopy and Transmission electron microscopy (TEM). The FT-IR spectroscopy was used to study the vibrations present in the prepared nanoparticles. The spectrum shows prominent bands at around 3300, 2853, 2890, 2924, 1383, 1650, 820 and 430–440 cm^{-1}; corresponding to H–O–H bending and O–H stretching vibrations of water molecules present on the surface of nanoparticles and the O–W–O asymmetric stretching vibration of the WO_4^{2-} tetrahedron. Characterization confirms single-phase formation, controlled morphology, and characteristic luminescence emission which can prove to be suitable for multicolour emission applications. The photoluminescence properties of the prepared nanoparticles were also studied and it is observed that by increasing the doping concentration of rare earth ions in the host i.e. $SrWO_4$, the emission intensity of the phosphors also increased and after reaching its optimum concentration, the luminescence intensity decreased drastically. For Eu^{3+} and Tb^{3+}, the optimum concentrations are 10 and 7 at. %, respectively.

1. Introduction

Alkaline-earth-metal tungstates AWO_4 (A = Ca, Sr, Ba) form a significant family of scheelite-type inorganic materials which are recognized for their structural stability and versatile optoelectronic properties [1–2]; showing wide applications in thermoluminescence, lasers and as excellent host material. Out of these alkaline-earth tungstates, $SrWO_4$ is an important electro-optical material which has an intrinsic strong blue emission band; however, its luminescence covers a broad range of wavelengths that are insensitive to external changes [3].

Over the past few decades, the luminescent properties of rare-earth ions have been the subject of extensive research due to their unique electronic configurations, specifically the rich energy level structures within the 4f orbitals, rare-earth materials exhibit diverse and abundant emission spectra [4]. Lanthanide-activated (Eu^{3+}, Tb^{3+}, Sm^{3+}, and Dy^{3+}) $SrWO_4$ phosphors are reported to produce sharp, characteristic red, green, and blue emissions, making them promising candidates for efficient LED and optical device applications. [5].

A major challenge in creating advanced luminescent materials is identifying optimal synthesis techniques to produce samples with high efficiency. To address this, various preparation methods have been developed, including solid-state reactions, hydrothermal synthesis, sol–gel processing, and template-directed methods etc. Other techniques include solvothermal-mediated microemulsions, as well as combining reverse micelle systems with dip-coating technology. [6–7]. Suitable organic-inorganic ligands can be used to tune the size and shape of the nanoparticles but long chain organic ligands cause quenching of luminescence due to high energy vibrations of the ligands. Long chain hydrocarbons such

as oleic acid, AOT, SDS etc. are not preferred as because they contain a number of O-H and C-H groups. Vibration of these groups lead to absorption of exciting light and non-radiative process occurs instead of radiative process. Synthetic methods employing high temperature could lead to agglomerated nanoparticles. This may cause decrease in luminescence intensity due to cross relaxation among Ln^{3+} ions. Therefore, in order to overcome the limitations encountered in these synthetic routes, efforts have been made to synthesize efficient phosphors with high luminescence intensity employing low temperature synthesis. When $SrWO_4$ are doped with lanthanide ions (Eu^{3+}, Tb^{3+}), they show their characteristic narrow red, green, and blue emissions and therefore these materials could serve as efficient phosphors in light emitting diode (LEDs) and other optical devices.

In the present work, $SrWO_4$: Eu^{3+}, $SrWO_4$: Tb^{3+} are prepared using ethylene glycol (EG) as the reaction medium; it also serves as the capping agent following the same reaction conditions as reported in my earlier works [8–12]. The luminescent properties of the synthesized nanoparticles are also studied in the present work.

2. Experimental details

2.1 Sample preparation

Nanoparticles of $SrWO_4$ doped with different RE^{3+} ions (Eu^{3+}, Tb^{3+}) were prepared using ethylene glycol as both capping agent and reaction medium and the temperature was maintained at 130 ^{o}C. Strontium nitrate ($Sr(NO_3)_2$), europium oxide (Eu_2O_3,99.99%, Aldrich), terbium nitrate hexahydrate ($Tb(NO_3)_3.6H_2O$, 99.99%, Aldrich), and sodium tungstate dihydrate ($Na_2WO_4.2H_2O$, AR) were used as sources of Ca^{2+}, Eu^{3+}, $Tb^{3+}$and WO_4^{2-}, respectively. Similar synthesis procedure was followed to prepare all the RE^{3+} doped samples by taking stoichiometric amounts of the starting materials as described in my earlier works.

The dried as prepared sample was then used for further characterization and luminescence studies.

2.2 Characterization

X-ray powder diffraction (XRD) data for all the samples were recorded using PANalytical powder diffractometer (X Pert PRO) with CuKα (1.5405 angstrom) radiation with Ni filter. The surface morphology of the samples was studied using CM-200 TEM (transmission electron microscopy). Infrared spectra were recorded on a Fourier transform infrared (FT-IR) spectrophotometer of Shimadzu (model 8400S) using thin pellets with KBr. UV-vis absorption spectrum was measured on Shimadzu (model 2450) spectrophotometer. All the photoluminescence spectra and lifetime measurements of the samples were recorded using Perkin Elmer (LS-55) luminescence spectrometer in phosphorescence mode with xenon discharge lamp as the excitation source having pulse width at half height < 10 μs.

3. Results and Discussion

3.1 XRD study

Figure 1 shows the XRD patterns of SrWO4 doped with different rare earth ions. The pattern shows well defined peaks and all these peaks could be indexed to the tetragonal phase of $SrWO_4$ with JCPDS card No. 01-085-0587 [13].

These powder phosphors fundamentally maintain characteristics of a scheelite structure which obviously are not affected by doped RE^{3+} ions [14]. The highest intensity peak is visible at $2\theta \approx 27^{o}$ (1 1 2). Figure 1 does not show any differences regarding scheelite diffraction patterns which indicate that doped RE^{3+} ions do not change the lattice structure. Due to different valence states and the difference in the ion size between W^{6+} (0.042 nm) and RE^{3+}, RE^{3+} are expected to occupy the Sr^{2+} (0.113 nm) site in this phosphor [15] which is reasonable because the electronic densities of RE^{3+} and Sr^{2+} at their coordination numbers are analogous [16]. No additional peaks for other phases have been found in all the patterns and this absence is strong verification of successful substitution of Sr^{2+} by the RE^{3+} ions in the tungstate framework.

The mean particle size of $SrWO_4$:RE^{3+} can be roughly determined from the broadening of peaks by using the Scherrer formula:

$d = 0.9\lambda/\beta\cos\theta$,

where λ is the wavelength of the X-ray and β is the full width at half maximum (FWHM).

For Eu^{3+} and Tb^{3+} doped samples, mean particle sizes are found to be 17 and 18 nm, respectively. The unit cell volume can be determined by calculating the cell parameters. The lattice parameters for 5 at. % Eu^{3+} is found to be a = 5.414, c = 11.96 and V = 350.564 and that for 15 at. % Tb^{3+} is a = 5.418, c = 11.90 and V = 349.321.

3.2 TEM study

Figure 2 shows the TEM images of Tb^{3+} and Eu^{3+} doped $SrWO_4$ nanoparticles. The majority of Tb^{3+} doped samples are spherical shaped (Fig. 2a), and the sizes are in the range of 15–23 nm in diameter. In addition to these, somewhat larger particles could also be seen. Eu^{3+} doped samples have particle size in the range of 21–30 nm; they do not have a regular shape; some are spherical while some are cubical (Fig. 2b).

3.3 FT-IR study

Figure 3 shows the FT-IR spectra for Eu^{3+} and Tb^{3+} doped $SrWO_4$ nanoparticles. The FT-IR spectrum shows prominent bands at around 3300, 2853, 2890, 2924, 1383, 1650, 820 and 430–440 cm^{-1}.

The bands at 1650 and 3300 cm^{-1} correspond to H–O–H bending and O–H stretching vibrations of water molecules present on the surface of nanoparticles, respectively [17].

The band at 820 cm^{-1} is due to the O–W–O asymmetric stretching vibration of the WO_4^{2-} tetrahedron and 440 cm^{-1} corresponds to the stretching vibration of W–O [18]. 1383 cm^{-1} vibration is due to the N–O band from HNO_3 used in the sample preparation. In the as-prepared sample peaks are observed at 2853 and 2924 cm^{-1} indicating C–H stretching vibration from EG molecules on the surface of $SrWO_4$:RE^{3+} nanoparticles.

3.4 Luminescence study

Figure 4a-b showed the excitation and emission spectra of $SrWO_4$: Tb^{3+} (7 at. %) nanoparticles prepared in EG. The excitation spectra were obtained by monitoring the emission of the Tb^{3+} $^5D_4$-$^7F_5$ transition at 546 nm. The excitation spectrum shows a broad band from 230 to 350 nm with its peak maximum at 238 nm. This peak maximum corresponds to oxygen-to-metal charge transfer (CTB) in tungstate [19]. This arises from the transition of 2*p* electrons of O^{2-} to the empty 5*d* shells of W^{6+} ions in the WO_4^{2-} group. Other bands observed from 350–450 nm are due to *f-f* transitions of rare-earth ions [20]. These peaks are weak compared to charge-transfer as *f-f* transitions are forbidden in nature.

The presence of the excitation band of the WO_4^{2-} groups in the excitation spectrum of Tb^{3+} indicates that there is an energy transfer from the WO_4^{2-} groups to Tb^{3+} ions in the $SrWO_4$:Tb^{3+} nanoparticles. Upon excitation into the WO_4^{2-} at 238 nm, the obtained emission spectrum contains the characteristic emission of Tb^{3+} with $^5D_4$-$^7F_5$ green emission (546 nm) as the most prominent group. In addition to this, some weaker emissions could also be observed and are located at 439, 491, 590 and 621 nm and they have been attributed to the transitions of $^5D_3 \rightarrow {}^7F_4$, $^5D_4 \rightarrow {}^7F_6$, $^5D_4 \rightarrow {}^7F_4$ and $^5D_4 \rightarrow {}^7F_3$, respectively.

The emission spectra shows that the luminescence intensity increases as the Tb^{3+} ion concentration is increased from 2 to 7 at. % and beyond this concentration, luminescence intensity decreases drastically. Thus, we can say that the optimum Tb^{3+} concentration for maximum luminescent intensity is 7 at. %. Above this particular concentration, the emission intensity decreases and this is due to concentration quenching effect. There is an increase in the dipole-dipole interaction with the increase in Tb^{3+} ion concentration eventually the cross- relaxation among Tb^{3+} ions increases when the mean distance between them is less than a critical value.

Similarly, for Eu^{3+} doped samples, the excitation spectrum (Fig. 5a-b) consists of a broad band at around 240 nm which can be attributed to the charge transfer within the WO_4^{2-} group [40–42]. Other weak peaks from 350–450 nm are also observed which may be due to *f-f* transitions of Eu^{3+} ion. Figure 5(a) shows the emission spectra for different concentrations of Eu^{3+} doped $SrWO_4$ samples. In the emission spectra, two prominent peaks are located at 595 nm (orange region) and 615 nm (red region). The 595

peak arises due to $^5D_1$-$^7F_1$ transition and 615 nm is due to $^5D_0$-$^7F_2$ transition. The electric dipole transition which is red in colour is dominant over orange transition.

From Fig. 5(b), it is also evident that the luminescence intensity varies with change in Eu^{3+} ion concentration. The intensity increases gradually with increase in rare-earth concentration from 5 at. % to 7 at. %, and further increases with up to 10 at. % of Eu^{3+} but beyond this concentration, the luminescence intensity decreases sharply. This phenomenon is due to the concentration quenching when the mean distance between the Eu^{3+}-Eu^{3+} is less than a critical value due to increased Eu^{3+} ion concentration. Thus, the optimum concentration for Eu^{3+} ion in $SrWO_4$ for highest intensity is 10 at. %.

This decrease in luminescence intensity after reaching a certain concentration of RE^{3+} is due to the quenching effect where reduced distance between activator ions increases nonradiative energy transfer [21]. Higher dopant ion concentration is not always favourable for phosphors and the need for knowing the optimum concentration of the dopant ion increases.

4. Conclusion

$SrWO_4$:RE^{3+} (RE = Eu, Tb) phosphors are prepared using ethylene glycol route. The synthesized samples possess a highly crystalline tetragonal structure. The size of the particles as determined from XRD study is around 20 nm. The shape of the prepared nanoparticles as seen from TEM images show that Tb^{3+} doped samples have spherical shape, Eu^{3+} are cubically as well as spherically shaped and the nanoparticles are well crystalline. FT-IR study shows bands at 820 cm^{-1} (which is due to the O–W–O asymmetric stretching vibration of the WO_4^{2-} tetrahedron) and 440 cm^{-1} (corresponding to the stretching vibration of W–O). From the excitation spectra, it is found that a broad band occurs from 230–350 nm with peak maximum at around 240 nm. This peak maximum corresponds to oxygen-to-metal charge transfer (CTB) in WO_4^{2-}. This arises from the transition of 2*p* electrons of O^{2-} to the empty 5*d* shells of W^{6+} ions in the WO_4^{2-} group. Other weaker bands observed from 350–450 nm are due to *f-f* transitions of rare-earth ions. These peaks are weak compared to charge-transfer as *f-f* transitions are forbidden in nature. For Eu^{3+} doped samples, characteristic emission lines are observed at 595 nm and 614 nm due to $^5D_1$-$^7F_1$ and $^5D_0$-$^7F_2$ transitions respectively; for Tb^{3+} doped samples, characteristic green emission could be observed at 546 nm due to $^5D_4$-$^7F_5$ transition. The luminescence intensity is again greatly influenced by the doping concentrations of the lanthanide ion, though no shift has been observed towards the higher or lower wavelength region by varying the doping concentration of dopant ion. For Eu^{3+} doped samples, the optimum concentration is found to be 10 at. %; for Tb^{3+} doped samples, the highest luminescence intensity is found to be 7 at. %.

Declarations

Ethica approval and consent to participate

Not applicable.

Competing interests

The authors declare no competing interests.

Funding

This research received no external funding.

Author Contribution

Dr. Kongbrailatpam Gayatri Sharma: Manuscript writing and reviewing, analysis and planning.

Acknowledgement

I acknowledge Dr. Th. Prasanta Singh, Chemistry Department, Standard College, Imphal, Manipur for reviewing the manuscript.

Data Availability

Data cannot be shared openly, but is available on request from the author.

References

1. Kazenas EK, Andreeva NA, Astakhova GK, Volchenkova VA, Ovchinnikova OA, Penkina TN, Fomina ON. Vapor composition and thermodynamic characteristics of gaseous molecules of alkaline earth metal tungstates. Inorg Mater Appl Res. 2024;15:893. https://doi.org/10.1134/S2075113324700357.
2. Hota SS, Panda D, Choudhary RNP. Studies of structural, dielectric, and electrical properties of polycrystalline barium bismuth tungstate for thermistor application. Inorg Chem Commun. 2023;153:110785. https://doi.org/10.1016/j.inoche.2023.110785.
3. Thongtem T, Kungwankunakorn S, Kuntalue B, Phuruangrat A, Thongtem S. Luminescence and absorbance of highly crystalline $CaMoO_4$, $SrMoO_4$, $CaWO_4$ and $SrWO_4$ nanoparticles synthesized by co-precipitation method at room temperature. J Alloys Compd. 2010;506:475. https://doi.org/10.1016/j.jallcom.2010.07.033.
4. Pereira PFS, Nogueira IC, Longo E, Nassar EJ, Rosa ILV, Cavalcante LS. Rietveld refinement and optical properties of $SrWO_4$:Eu^{3+} powders prepared by the non-hydrolytic sol-gel method. J Rare Earths. 2015;33:113. https://doi.org/10.1016/S1002-0721(14)60391-4.

5. Maheshwary, Singh BP, Singh RA. Effect of annealing on the structural, optical and emissive properties of $SrWO_4$:Ln^{3+} (Dy^{3+}, Eu^{3+} and Sm^{3+}). Nanopart Spectrochim Acta Mol Biomol Spectrosc. 2016;152:199. https://doi.org/10.1016/j.saa.2015.07.074.
6. Zheng Y, Lin X, Wang Q, Cai W, Zhang CC. Dibenzoyl-L-cystine as organic directing agent for assembly of visible-light-sensitized luminescent AgGd $(MoO_4)_2$: Eu^{3+} nanowires. Mat Res Bull. 2012;47(3):856. https://doi.org/10.1016/j.materresbull.2011.11.045.
7. Kumari S, Rao AS, Sinha RK. Structural and photoluminescence properties of Sm^{3+} ions doped strontium yttrium tungstate phosphors for reddish-orange photonic device applications. Mat Res Bull. 2023;167:112419. https://doi.org/10.1016/j.materresbull.2023.112419.
8. Sharma KG, Singh NR. Synthesis of $CaWO_4$:Eu^{3+} phosphor powders via ethylene glycol route and its optical properties. J Rare Earths. 2012;30:310. https://doi.org/10.1016/S1002-0721(12)60043-X.
9. Sharma KG, Singh NR. Re-dispersible $CaWO_4$:Tb^{3+} nanoparticles: Synthesis, characterization and photoluminescence studies. J Lumin. 2013;139:98. https://doi.org/10.1016/j.jlumin.2013.02.006.
10. Sharma KG, Singh NR. Synthesis and luminescence properties of $CaMO_4$:Dy^{3+}(M = W, Mo) nanoparticles prepared via an ethylene glycol route. New J Chem. 2013;37:2784. https://doi.org/10.1039/C3NJ00155E.
11. Sharma KG, Singh TP, Singh NR. Low temperature synthesis, characterization and tunable optical properties of Eu^{3+}, Tb^{3+} doped $CaMoO_4$ nanoparticles. J Alloys Compd. 2014;602:275. https://doi.org/10.1016/j.jallcom.2014.02.186.
12. Sharma KG, Singh NS, Devi YR, Singh NR, Singh SD. Effects of annealing on luminescence of $CaWO_4$: Eu^{3+} nanoparticles and its thermoluminescence study. J Alloys Compd. 2013;556:94. https://doi.org/10.1016/j.jallcom.2012.12.087.
13. Potanina EA, Orlova AI, Mikhailov DA, Nokhrin AV, Chuvil'deev VN, Boldin MS, Sakharov NV, Lantcev EA, Tokarev MG, Murashov AA. Spark plasma sintering of fine-grained $SrWO_4$ and $NaNd(WO_4)_2$ tungstates ceramics with the scheelite structure for nuclear waste immobilization. J Alloys Compd. 2019;774:182. https://doi.org/10.1016/j.jallcom.2018.09.348.
14. Zhou L, Wei J, Wu J, Gong F, Yi L, Huang J. Potential red-emitting phosphor for white LED solid-state lighting. J Alloys Compd. 2009;476:390. https://doi.org/10.1016/j.jallcom.2008.09.005.
15. He X, Guan M, Lian N, Sun J, Shang T. Synthesis and luminescence characteristics of K_2Bi (PO_4) (MO_4): Eu^{3+} (M = Mo, W) red-emitting phosphor for white LEDs. J Alloys Compd. 2010;492:452. https://doi.org/10.1016/j.jallcom.2009.11.138.
16. Sivaganesh D, Saravanakumar S, Sivakumar V, Sasikumar S, Gopal JN, Kalpana S, Rajajeyaganthan R. Sm^{3+} induced-$SrWO_4$ phosphor: analysis of photoluminescence and photocatalytic properties with electron density distribution studies. J Mater Sci: Mater Electron. 2020;31:8865. https://doi.org/10.1007/s10854-020-03421-8.

17. Seki T, Chiang KY, Yu CC, Yu X, Okuno M, Hunger J, Nagata Y, Bonn M. The bending mode of water: a powerful probe for hydrogen bond structure of aqueous systems. J Phys Chem Lett. 2020;11:8459. https://doi.org/10.1021/acs.jpclett.0c01259.
18. Azevêdo HV, da Silva EBS, Fernandes RS, Albuquerque AR, Gomes UU, Cavalcante DG. Green chemistry synthesis of wolframites: An investigation about stoichiometric ratios, optical, structural, vibrational, and physico-chemical properties. J Clean Prod. 2023;385:35528. https://doi.org/10.1016/j.jclepro.2022.135528.
19. Alexander D, Kumar BR, Mathews JM. Spectroscopic analysis of calcium tungstate and Eu doped calcium tungstate phosphor. Mater Today Proc. 2023.https://doi.org/10.1016/j.matpr.2023.11.129
20. Hasegawa M, Ohmagari H, Tanaka H, Machida K. Luminescence of lanthanide complexes: From fundamental to prospective approaches related to water-and molecular-stimuli. J Photochem Photobiol C Photochem Rev.2022;50:100484.https://doi.org/10.1016/j.jphotochemrev.2022.100484
21. Sun L, Gao R, Pan T, Ai XC, Fu L, Zhang JP. Concentration-regulated photon upconversion and quenching in $NaYF_4$: Yb^{3+}, Er^{3+} nanocrystals: nonexponentiality revisited. Nanoscale. 2019;11:18150. https://doi.org/10.1039/C9NR06521K.

Figures

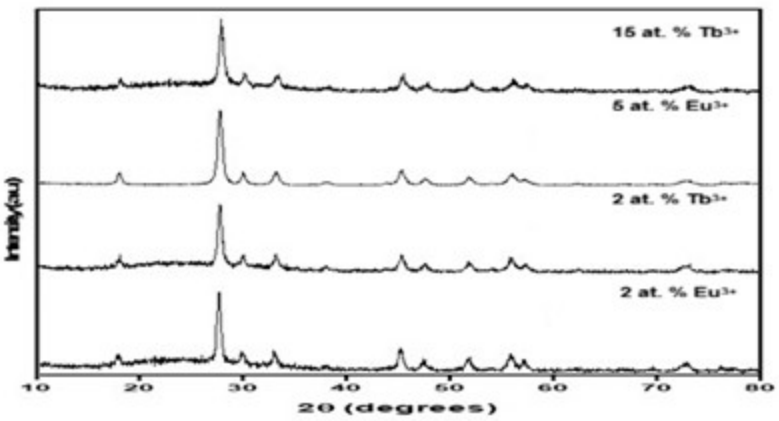


Figure 1

XRD patterns of RE^{3+} doped $SrWO_4$ nanoparticles.

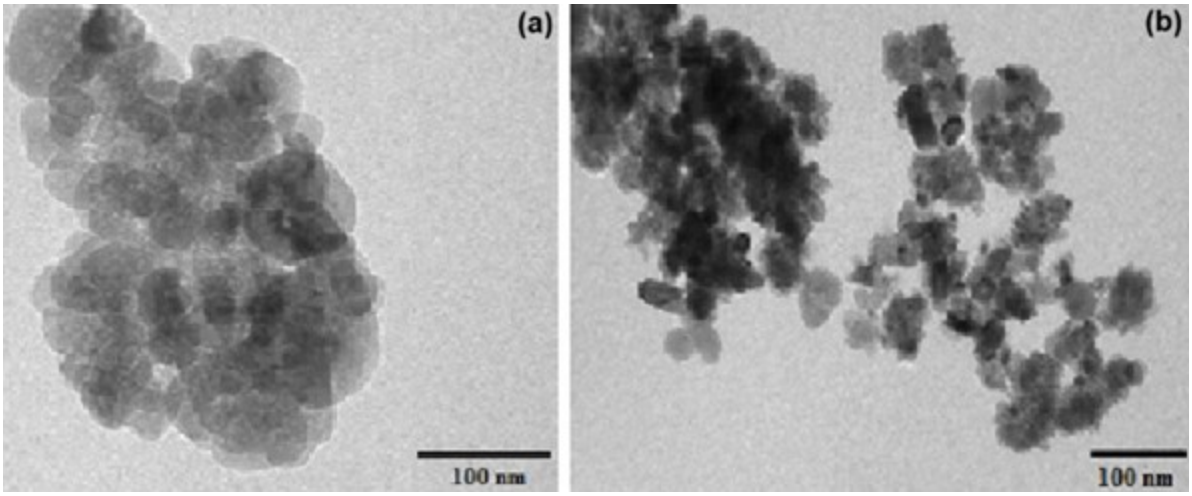


Figure 2

TEM images of (a) 7 at. % Tb^{3+} and (b) 5 at. % Eu^{3+}.

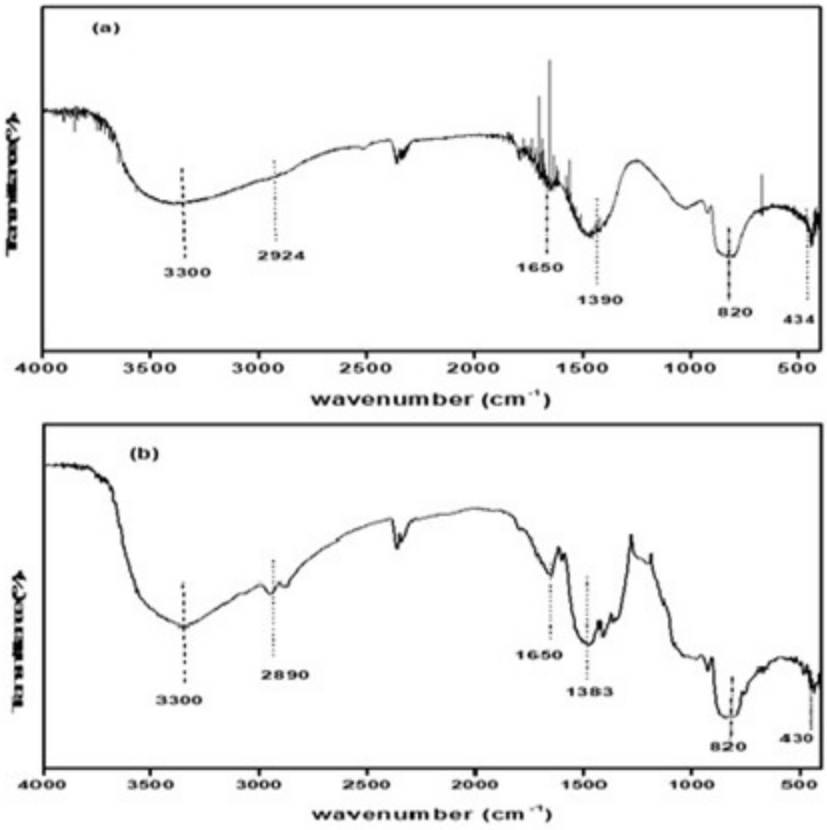


Figure 3

FT-IR spectra for (a) 5 at. % Eu^{3+} and (b) 7 at. % Tb^{3+} doped $SrWO_4$ nanoparticles.

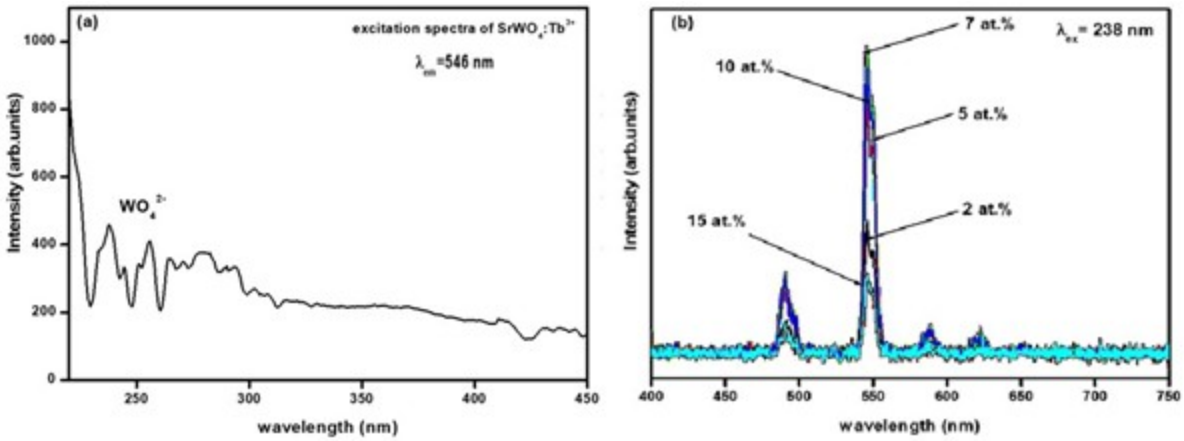


Figure 4

(a) Excitation and (b) emission spectra for $SrWO_4:Tb^{3+}$ nanoparticles prepared in EG.

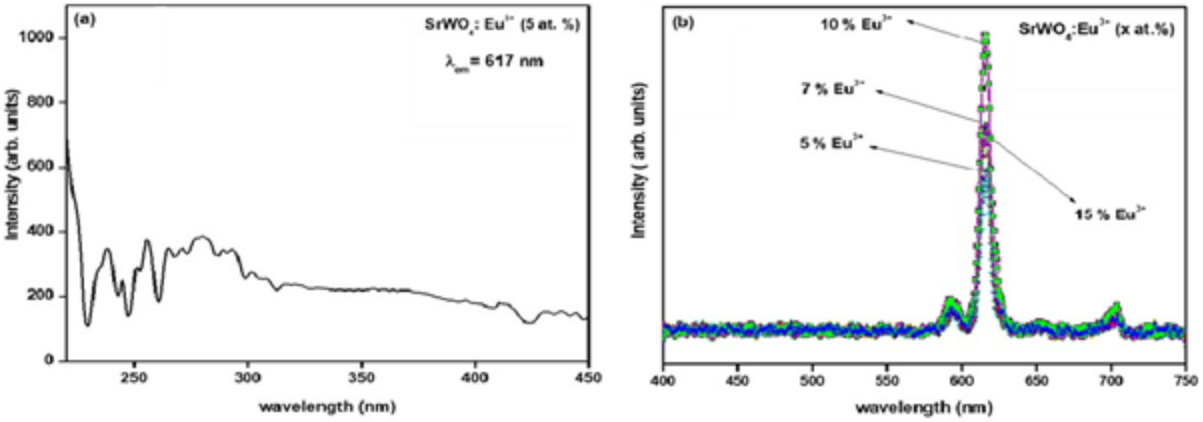


Figure 5

(a) Excitation and (b) emission spectra of $SrWO_4:Eu^{3+}$ nanoparticles in EG.